Optical dichroism: E1–M1 integral relations

2006 J. Phys. A: Math. Gen. 39 1969

(http://iopscience.iop.org/0305-4470/39/8/013)

INSTITUTE OF PHYSICS PUBLISHING JOURNAL OF PHYSICS A: MATHEMATICAL AND GENERAL

J. Phys. A: Math. Gen. **39** (2006) 1969–1978 doi:10.1088/0305-4470/39/8/013

Optical dichroism: E1–M1 integral relations

Ivan Marri[1], **Paolo Carra**[2,3] **and C M Bertoni**[1]

[1] S[3] INFM-CNR and Physics Department, University of Modena and Reggio Emilia, 41100 Modena, Italy
[2] European Synchrotron Radiation Facility, B.P. 220, F-38043 Grenoble Cédex, France

E-mail: marri@unimo.it, carra@esrf.fr and bertoni@unimo.it

Received 30 September 2005
Published 8 February 2006
Online at stacks.iop.org/JPhysA/39/1969

Abstract

The present paper discusses optical dichroism in noncentrosymmetric systems. The cases of circular and linear polarizations are considered. Integrated spectra are interpreted using effective two-electron operators, which are derived within a localized (atomic) model. As a consequence, our theory is not suitable for quantitative predictions; nevertheless, it identifies microscopic origins of natural, nonreciprocal and Jones' dichroisms.

PACS numbers: 78.40.−q, 78.20.Ek, 78.20.Fm

1. Introduction

In condensed-matter systems, effects of space-inversion symmetry breaking can be described by space-odd order parameters, which are specified using spin and orbital irreducible tensors. They are investigated by a variety of spectroscopies ranging from optics to x rays.

X-ray experiments, primarily absorption with its various forms of dichroism, are performed with synchrotron radiation, exploiting photon polarization and energy tunability. Two features characterize these inner-shell x-ray spectroscopies: crystal-site selectivity (from energy tuning) and angular-momentum resolution (from selection rules). Sensitivity to space-odd order parameters is obtained by picking out an interference between electric-dipole and electric-quadrupole excitations (Alagna *et al* 1998, Goulon *et al* 1998, Natoli *et al* 1998, Goulon *et al* 2000, 2002). Recording a non-vanishing E1–E2 spectrum thus requires an ordered structure. Using an atomic approximation, theoretical work has identified a set of physical observables, which are probed by these experiments (Carra *et al* 2003, Marri and Carra 2004).

In the optical region, several phenomena arising from the breaking of space inversion have also been observed:

[3] Dr Paolo Carra unexpectedly died on 18 October 2005 at the age of 53. The coauthors remember their great friend and his life dedicated to Science.

- *Natural optical activity*, i.e., a difference in absorption between right- and left-circularly polarized photons, or rotation of the polarization plane, in a nonmagnetic system (Barron 1982).
- *Magnetochiral anisotropy*, i.e., a shift in the refractive index (or dichroism in the absorption coefficient) of a chiral medium, when the photon beam is collinear with an external applied magnetic field; the sign of the shift changes when the relative direction between field and beam is inverted, or when, for a given relative direction, one switches from one chiral medium to its enantiomer (Wagnier and Meier 1982).
- *Magnetoelectric dichroism*, observed in magnetoelectric crystals with or without the application of external electric and magnetic fields (Jones 1948, Wagnier and Meier 1982, Krichevtsov *et al* 1996, Roth and Rikken 2000 and 2002, Jung *et al* 2004).

These optical effects are mainly ascribed to an interference between electric-dipole and magnetic-dipole (E1–M1) excitations. Nonvanishing spectra can thus be recorded also in disordered systems.

The aim of this paper is to report an analytic study of the E1–M1 absorption cross section, as a function of photon polarization and wave vector. Circular and linear dichroism and anisotropies will be analysed. Our theory is based on tensor methods (Racah calculus), which are implemented within a single-ion model. For inner-shell excitations, corrections to this atomic approximation have been calculated using orthonormal LMTOs as a one-particle basis for electron band states (Benoist *et al* 2000). In this framework, integrated dichroic spectra are given by a one-particle atomic contribution (leading order) followed by a series of terms, which can be expressed in the form of energy moments of the valence band. By leaving a localized core hole, x-ray absorption selects a specific site in the solid. A local process is thus expected to control the excitation. Corrections are small, in general, and the atomic approximation works well. This is not the case for optical excitations. Visible and ultraviolet light probe the sample on the length scale from 1 μm to a few nanometres. The process is obviously non-local, rendering the single-ion model irrealistic for quantitative predictions.

On the other hand, the problem of identifying the microscopic origin of optical dichroism in noncentrosymmetric systems remains and multi-site analytical calculations appear to be out of reach at present. We have thus performed a single-site analysis. As explained in the remaining sections of this paper, this local approximation yields integrated spectra as a linear combination of (one-site) two-particle effective electron operators with a well-defined physical meaning, thus elucidating the microscopic nature of optical parity-breaking phenomena.

2. E1–M1 absorption cross section

We consider the absorption cross section

$$\sigma^{\boldsymbol{\epsilon}}_{\mathrm{E1-M1}}(\omega) = \frac{2\pi^2\alpha\hbar\omega}{mc}\left[\sum_{\iota,\iota',f}\langle g|\boldsymbol{\epsilon}^*\cdot\mathbf{r}_\iota|f\rangle\langle f|(\boldsymbol{\epsilon}\times\hat{\mathbf{k}})\cdot\mathbf{l}_{\iota'}|g\rangle + \mathrm{c.c.}\right] \times \delta(E_f - E_g - \hbar\omega), \tag{1}$$

which selects the E1–M1 interference (to leading order) in the $\mathbf{p}\cdot\mathbf{A}$ interaction between photons and electrons. Here, $\hbar\omega$, $\hat{\mathbf{k}} = \mathbf{k}/k$ and $\boldsymbol{\epsilon}$ represent energy, wave-vector direction and polarization of the photon; $|g\rangle$ and $|f\rangle$ denote ground and final states of the electron system, with energies E_g and E_f, respectively; electrons are labelled by ι and ι'; $\alpha = e^2/\hbar c$ and $\mathbf{l} = \hbar^{-1}\mathbf{L}$ stands for a dimensionless orbital angular momentum.

Our study centres on the integrated intensity

$$\Sigma_{\mathrm{E1\text{–}M1}}(\boldsymbol{\epsilon}) = \int \frac{\sigma^{\boldsymbol{\epsilon}}_{\mathrm{E1\text{–}M1}}}{\hbar\omega}\,\mathrm{d}(\hbar\omega), \tag{2}$$

where integration is over a finite energy interval, which is relevant for optical spectra[4]. Equation (2) expands into a linear combination of pairs of tensors of increasing rank, $r = 0$, 1 and 2. Each pair is given by the scalar product of a *geometrical factor* (a wave-vector and polarization response) and the ground-state expectation value of an *effective electron operator*. We will now proceed to the derivation of this expansion.

Our method hinges on the second-quantization formalism. We introduce the fermionic field

$$\Psi(\mathbf{r}) = \sum_{l\lambda\sigma} a_{l\lambda\sigma}\,\psi_{l\lambda\sigma}(\mathbf{r}), \tag{3}$$

where $a_{l\lambda\sigma}$ annihilates a valence electron, which is labelled by orbital quantum number l, λ and spin σ. Valence states are identified by uncoupled spin-orbital wave functions

$$\psi_{l\lambda\sigma}(\mathbf{r}) = \phi_l(r)\,Y_{l\lambda}(\hat{\mathbf{n}})\,\chi_\sigma, \tag{4}$$

with $\hat{\mathbf{n}} = \mathbf{r}/r$. In this one-electron basis, equation (1) takes the form

$$\begin{aligned}\sigma^{\boldsymbol{\epsilon}}_{\mathrm{E1\text{–}M1}} = \frac{2\pi^2\alpha\hbar\omega}{mc}\Bigg[&\sum_f \sum_{\substack{l\lambda\sigma\\ l'\lambda'\sigma'}} \sum_{\substack{l_1\lambda_1\sigma_1\\ l_2\lambda_2\sigma_2}} \langle\psi_{l'\lambda'\sigma'}(\mathbf{r})|\boldsymbol{\epsilon}^*\cdot\mathbf{r}|\psi_{l\lambda\sigma}(\mathbf{r})\rangle\\ &\times\left\langle\psi_{l_1\lambda_1\sigma_1}(\mathbf{r})\right|(\boldsymbol{\epsilon}\times\hat{\mathbf{k}})\cdot\mathbf{l}\left|\psi_{l_2\lambda_2\sigma_2}(\mathbf{r})\right\rangle\langle g|a^\dagger_{l'\lambda'\sigma'}a_{l\lambda\sigma}|f\rangle\\ &\times\langle f|a^\dagger_{l_1\lambda_1\sigma_1}a_{l_2\lambda_2\sigma_2}|g\rangle + \mathrm{c.c.}\Bigg]\,\delta(E_f - E_g - \hbar\omega),\end{aligned} \tag{5}$$

where $l' = l \pm 1$. We insert equation (5) into equation (2) and apply the Wigner–Eckart theorem. After some algebra, we find

$$\begin{aligned}\Sigma_{\mathrm{E1\text{–}M1}}(\boldsymbol{\epsilon}) = \frac{8\mathrm{i}\sqrt{2}\pi^2\alpha}{mc}\Bigg[&\sum_{\substack{r\\ \alpha\beta\rho}} \sum_{\substack{l_1\lambda_1\lambda_2\\ l\lambda l'\lambda'}} R^1_{ll'}R^0_{l_1l_1}(-1)^\rho[(2l+1)l_1(l_1+1)]^{\frac{1}{2}}\\ &\times C^{l'0}_{l0;10}C^{r\rho}_{1\alpha;1\beta}\Bigg(\mathcal{S}^r_{-\rho}(\boldsymbol{\epsilon},\boldsymbol{\epsilon}^*,\hat{\mathbf{k}})\frac{C^{l'\lambda'}_{l\lambda;1\alpha}C^{l_1\lambda_1}_{l_1\lambda_2;1\beta}}{\sqrt{2l'+1}}\langle g|a^\dagger_{l'\lambda'}a_{l\lambda}a^\dagger_{l_1\lambda_1}a_{l_1\lambda_2}|g\rangle\\ &\times(-1)^{r+1}\mathcal{Q}^r_{-\rho}(\boldsymbol{\epsilon},\boldsymbol{\epsilon}^*,\hat{\mathbf{k}})\frac{C^{l_1\lambda_2}_{l_1\lambda_1;1\alpha}C^{l\lambda}_{l'\lambda';1\beta}}{\sqrt{2l+1}}\langle g|a^\dagger_{l_1\lambda_2}a_{l_1\lambda_1}a^\dagger_{l\lambda}a_{l'\lambda'}|g\rangle\Bigg)\Bigg],\end{aligned} \tag{6}$$

where the radial integrals are given by $R^L_{ll'} = \int_0^\infty \mathrm{d}r\phi_l(r)r^{L+2}\phi_{l'}$; $C^{c\gamma}_{a\alpha;b\beta}$ denotes a Clebsch–Gordan coefficient. The geometrical factors $\mathcal{S}^r_{-\rho}$ and $\mathcal{Q}^r_{-\rho}$ are defined by

$$\mathcal{S}^r_{-\rho}(\boldsymbol{\epsilon},\boldsymbol{\epsilon}^*,\hat{\mathbf{k}}) = \sum_{\substack{q\nu\mu\\ p\kappa}} \sqrt{3(2p+1)}\begin{Bmatrix}1 & 1 & p\\ 1 & r & 1\end{Bmatrix} C^{p\kappa}_{1-q;1\nu}C^{r-\rho}_{p\kappa;1\mu}\boldsymbol{\epsilon}^*_{-q}\boldsymbol{\epsilon}_\nu\hat{\mathbf{k}}_\mu \tag{7}$$

[4] The energy range of interest covers intra-band transions in the optical region. In our derivation, the valence states $j_\pm = l \pm \frac{1}{2}$ are assumed to be degenerate. Absorption is sensitive to purely orbital electronic properties in this case. Spin-dependent terms are included by extending the theory according to the method of Marri and Carra (2004).

with

$$\mathcal{Q}^r(\boldsymbol{\epsilon}, \boldsymbol{\epsilon}^*, \hat{\mathbf{k}}) = \mathcal{S}^r(\boldsymbol{\epsilon}, \boldsymbol{\epsilon}^*, \hat{\mathbf{k}}), \quad \text{when } \boldsymbol{\epsilon} \text{ is real,} \tag{8}$$

and

$$\mathcal{Q}^r(\boldsymbol{\epsilon}, \boldsymbol{\epsilon}^*, \hat{\mathbf{k}}) = S^r(\boldsymbol{\epsilon}^*, \boldsymbol{\epsilon}, \hat{\mathbf{k}}) \quad \text{when } \boldsymbol{\epsilon} \text{ is complex.} \tag{9}$$

Equation (6) provides the required expansion of the integrated intensity into a linear combination of coupled tensors[5]. Selection of appropriate photon polarization and wave vector affords a study of integrated dichroic spectra and their dependence on microscopic electronic properties of the sample, as described below. (Mathematical details about the derivation of equation (6) are given in the appendix.)

3. Optical natural circular dichroism

Optical natural circular dichroism (ONCD) measures the difference in absorption between right (−) and left (+) circularly polarized photons, which are defined by $\boldsymbol{\epsilon}^{\pm} = \mp(\mathrm{i}/\sqrt{2})(\boldsymbol{\epsilon}_1 \pm \mathrm{i}\boldsymbol{\epsilon}_2)$. We therefore consider the integrated intensity

$$\begin{aligned}\Sigma^{\mathrm{OCND}}_{\mathrm{E1\text{–}M1}} &= \Sigma_{\mathrm{E1\text{–}M1}}(\boldsymbol{\epsilon}^-) - \Sigma_{\mathrm{E1\text{–}M1}}(\boldsymbol{\epsilon}^+) \\ &= \int \frac{\sigma^{\boldsymbol{\epsilon}^-}_{\mathrm{E1\text{–}M1}} - \sigma^{\boldsymbol{\epsilon}^+}_{\mathrm{E1\text{–}M1}}}{\hbar\omega}\, \mathrm{d}(\hbar\omega),\end{aligned} \tag{10}$$

and work out the corresponding geometrical factors and effective electron operators. *Geometrical factors*. Expression (10) contains the combinations

$$\begin{aligned}\mathcal{S}^r_\rho(\boldsymbol{\epsilon}, {}^-\, \boldsymbol{\epsilon}^+, \hat{\mathbf{k}}) - \mathcal{S}^r_\rho(\boldsymbol{\epsilon}^+, \boldsymbol{\epsilon}^-, \hat{\mathbf{k}}) &= -\left[\mathcal{Q}^r_\rho(\boldsymbol{\epsilon}, {}^-\, \boldsymbol{\epsilon}^+, \hat{\mathbf{k}}) - \mathcal{Q}^r_\rho(\boldsymbol{\epsilon}^+, \boldsymbol{\epsilon}^-, \hat{\mathbf{k}})\right] \\ &\equiv T^r_\rho(\boldsymbol{\epsilon}^-, \boldsymbol{\epsilon}^+, \hat{\mathbf{k}})_{\mathrm{ONCD}},\end{aligned} \tag{11}$$

which do not vanish only when $p = 1$, as inferred from equations (7) and (9). When $r = 1$, $T^1_{\mathrm{OCND}} \propto (\boldsymbol{\epsilon} \times \boldsymbol{\epsilon}^*) \times \hat{\mathbf{k}} = 0$, for transverse waves. Only the values $r = 0, 2$ contribute therefore to equation (10). Explicitly

$$T^0_0(\boldsymbol{\epsilon}^-, \boldsymbol{\epsilon}^+, \hat{\mathbf{k}})_{\mathrm{ONCD}} = \mathrm{i}\frac{2}{\sqrt{6}}(\boldsymbol{\epsilon}^+ \times \boldsymbol{\epsilon}^-) \cdot \hat{\mathbf{k}} = -\frac{2}{\sqrt{6}}$$

and

$$T^2_\rho(\boldsymbol{\epsilon}^-, \boldsymbol{\epsilon}^+, \hat{\mathbf{k}})_{\mathrm{ONCD}} = \frac{\mathrm{i}}{\sqrt{2}}[\boldsymbol{\epsilon}^+ \times \boldsymbol{\epsilon}^-, \hat{\mathbf{k}}]^2_\rho.$$

(Tensor couplings are defined by means of Clebsch–Gordan coefficients: $[U^p, V^q]^z_\eta \equiv \sum_{\mu\nu} C^{z\eta}_{p\mu;q\nu} U^p_\mu V^q_\nu$.) Equation (10) can thus be cast in the following form

$$\begin{aligned}\Sigma^{\mathrm{ONCD}}_{\mathrm{E1\text{–}M1}} = {} & \frac{\mathrm{i}8\sqrt{2}\pi^2\alpha}{mc} \sum_{ll'l''}^{r} R^1_{ll'} R^0_{l'l''} \sqrt{(2l+1)l''(l''+1)} \\ & C^{l'0}_{l0,10} \sum_\rho (-1)^\rho T^r_{-\rho}(\boldsymbol{\epsilon}^-, \boldsymbol{\epsilon}^+, \hat{\mathbf{k}})_{\mathrm{ONCD}} \langle g | F^r_\rho(\omega)^{l,l',l''}_{\mathrm{ONCD}} | g \rangle,\end{aligned} \tag{12}$$

[5] Only totally symmetric representations of the transition operator will contribute to $\Sigma_{\mathrm{E1\text{–}M1}}(\boldsymbol{\epsilon})$ (Carra and Thole 1994).

with

$$F^r_\rho(\omega)^{l,l',l''}_{\mathrm{ONCD}} = \sum_{\substack{\alpha\beta \\ \lambda\lambda'\lambda_1\lambda_2}} C^{r\rho}_{1\alpha,1\beta}\left[\frac{C^{l'\lambda'}_{l\lambda,1\alpha}C^{l''\lambda_1}_{l''\lambda_2,1\beta}a^\dagger_{l'\lambda'}a_{l\lambda}a^\dagger_{l''\lambda_1}a_{l''\lambda_2}}{\sqrt{2l'+1}} + \frac{C^{l''\lambda_2}_{l''\lambda_1,1\alpha}C^{l\lambda}_{l'\lambda',1\beta}a^\dagger_{l''\lambda_2}a_{l''\lambda_1}a^\dagger_{l\lambda}a_{l'\lambda'}}{\sqrt{2l+1}}\right], \tag{13}$$

which identifies the electron operators in $\Sigma^{\mathrm{OCND}}_{\mathrm{E1-M1}}$.

Effective electron operators. We will now show that equation (13) can be rewritten in terms of two-particle effective electron operators (irreducible tensors). These tensors are constructed using the following basic operators: the angular momentum $\mathbf{l}$; the shift operators $\mathbf{A} = \mathbf{n}f_1(N_0) + \nabla_\Omega f_2(N_0)$ and $\mathbf{A}^\dagger$, with $\nabla_\Omega = -\mathrm{i}\mathbf{n}\times\mathbf{l}$, $f_1(N_0) = \left(N_0 - \frac{1}{2}\right)f_2(N_0)$ and $f_2(N_0) = \sqrt{(N_0-1)/N_0}$; and N_0, which is defined by $N_0|lm\rangle = \left(l+\frac{1}{2}\right)|lm\rangle$, with $|lm\rangle$ being a spherical harmonic. When acting onto $|lm\rangle$, $\mathbf{A}$ and $\mathbf{A}^\dagger$ change l into $l-1$ and $l+1$, respectively. We will also consider the linear combinations: $\mathbf{A}^- = \mathrm{i}(\mathbf{A}-\mathbf{A}^\dagger)\sqrt{2}$ and $\mathbf{A}^+ = \mathrm{i}(\mathbf{A}+\mathbf{A}^\dagger)\sqrt{2}$. The vector $\mathbf{n}$ identifies the direction of electric polarization.

Within this formalism, we find

$$F^r_\rho(\omega)^{l,l'=l-1,l''}_{\mathrm{ONCD}} = \frac{\sqrt{2l''+1}}{\langle l'\|\mathbf{A}\|l\rangle\langle l''\|\mathbf{l}\|l''\rangle}\sum_{\alpha\beta}\sum_{\lambda\lambda'\lambda_1\lambda_2} C^{r\rho}_{1\alpha;1\beta} \times\left[\langle l'\lambda'|A_\alpha|l\lambda\rangle a^\dagger_{l'\lambda'}a_{l\lambda}\langle l''\lambda_1|l_\beta|l''\lambda_2\rangle a^\dagger_{l''\lambda_1}a_{l''\lambda_2} + \mathrm{h.c.}\right], \tag{14}$$

for the case $l' = l-1$. A similar expression is derived for $l' = l+1$. Defining space-odd one-electron operators

$$\sum_\iota\left[\mathcal{O}^r_{\iota,\rho}\right]^{l,l'} = \sum_{\lambda\lambda'}\langle l'\lambda'|\mathcal{O}^r_\rho|l\lambda\rangle a^\dagger_{l'\lambda'}a_{l\lambda} + \mathrm{h.c.}, \tag{15}$$

we couple them and form two-particle irreducible tensors, so that

$$F^r_\rho(\omega)^{l,l'=l-1,l''}_{\mathrm{ONCD}} = \frac{\sqrt{2l'+1}}{\langle l'\|\mathbf{A}\|l\rangle\langle l'\|\mathbf{l}\|l'\rangle}\sum_{\iota\iota'}\left([\mathbf{A}_\iota,\mathbf{l}_{\iota'}]^r_\rho - [\mathbf{l}_{\iota'},\mathbf{A}_\iota]^r_\rho\right)^{l,l'=l-1,l''}. \tag{16}$$

Again, a similar expression for $l' = l+1$ is obtained. Using the following one-particle relations (Carra 2001)

$$\langle l'm'|\mathrm{i}\mathbf{A}^-|lm\rangle = \frac{\sqrt{(2l+1)(2l'+1)}}{l+l'+1}\frac{1}{\sqrt{2}}\langle l'm'|\mathbf{n}\times\mathbf{l}-\mathbf{l}\times\mathbf{n}|lm\rangle \tag{17}$$

and (Carra *et al* 2003)

$$\Omega^L = \frac{\mathbf{n}\times\mathbf{l}-\mathbf{l}\times\mathbf{n}}{2} = \frac{1}{2}\frac{1}{\sqrt{N_0}}[N_0,\mathbf{A}^-]_+\frac{1}{\sqrt{N_0}}, \tag{18}$$

$$\mathbf{A}^+ = \sqrt{N_0}\mathbf{n}\sqrt{N_0}, \tag{19}$$

we finally obtain

$$\Sigma^{\mathrm{ONCD}}_{\mathrm{E1-M1}} = \Sigma_{\mathrm{E1-M1}}(\boldsymbol{\epsilon}^-) - \Sigma_{\mathrm{E1-M1}}(\boldsymbol{\epsilon}^+) = -\frac{8\sqrt{2}\pi^2\alpha}{mc}\sum a_{l,l'}R^1_{ll'}R^0_{l''l''} \times\left[\frac{1}{\sqrt{3}}T^0_0(\boldsymbol{\epsilon}^-,\boldsymbol{\epsilon}^+,\hat{\mathbf{k}})_{\mathrm{ONCD}}\sum_{\substack{\iota\iota' \\ \iota\neq\iota'}}\langle g|\Omega^L_\iota\cdot\mathbf{l}_{\iota'}|g\rangle\right.$$

$$-\sum_{\rho}(-1)^{\rho}T^{2}_{-\rho}(\boldsymbol{\epsilon}^{-},\boldsymbol{\epsilon}^{+},\hat{\mathbf{k}})_{\mathrm{ONCD}}\sum_{u'}\langle g|\left[\Omega^{L}_{t},\mathbf{l}_{t'}\right]^{2}_{\rho}|g\rangle\Bigg], \tag{20}$$

with

$$a_{l,l'}=\frac{2(l'-l)}{l+l'+1}.$$

The vector operator Ω^{L} is known as (one-particle) *orbital anapole*.

Equation (20) is our main result for natural circular dichroism in the optical region. It provides a microscopical interpretation of integrated ONCD spectra in terms of two effective electron operators: an *orbital pseudoscalar* and an *orbital pseudodeviator*. Note that these tensors are two-particle electron operators, as they stem from valence excitations. This should be contrasted with x-ray natural dichroism where one-electron properties are probed (Carra *et al* 2003). The orbital pseudoscalar can distinguish between enantiomeric and nonenantiomeric systems; indeed, it averages to zero when the permitted point group contains a mirror plane as a symmetry operation[6]. The orbital pseudodeviator represents the two-particle generalization of the rank-2 tensor probed by x-ray natural dichroism. A one-particle pseudodeviator can be viewed as the space-odd analogue of a charge quadrupole. In equation (20), both electron operators have *polar* symmetry, i.e., they are space odd and time even.

4. Optical non-reciprocal linear dichroism

This section derives an integral relation for E1–M1 optical nonreciprocal linear dichroism (ONLD), which measures the difference in absorption between two different linearly-polarized photons, denoted by $\boldsymbol{\epsilon}'$ and $\boldsymbol{\epsilon}''$[7]. We consider the expression

$$\Sigma^{\mathrm{ONLD}}_{\mathrm{E1\text{–}M1}}=\int\frac{\sigma^{\boldsymbol{\epsilon}'}_{\mathrm{E1\text{–}M1}}-\sigma^{\boldsymbol{\epsilon}''}_{\mathrm{E1\text{–}M1}}}{\hbar\omega}=\Sigma_{\mathrm{E1\text{–}M1}}(\boldsymbol{\epsilon}')-\Sigma_{\mathrm{E1\text{–}M1}}(\boldsymbol{\epsilon}'') \tag{21}$$

and, as in the previous case, we will determine the geometrical factors and effective electron operators.

Geometrical factor. Equation (21) contains the terms

$$\begin{aligned}\mathcal{S}^{r}_{\rho}(\boldsymbol{\epsilon}',\hat{\mathbf{k}}')-\mathcal{S}^{r}_{\rho}(\boldsymbol{\epsilon}'',\hat{\mathbf{k}}'')&=\mathcal{Q}^{r}_{\rho}(\boldsymbol{\epsilon}',\hat{\mathbf{k}}')-\mathcal{Q}^{r}_{\rho}(\boldsymbol{\epsilon}'',\hat{\mathbf{k}}'')\\&=T^{r}_{\rho}(\boldsymbol{\epsilon}',\hat{\mathbf{k}}',\boldsymbol{\epsilon}'',\hat{\mathbf{k}}'')_{\mathrm{ONLD}}.\end{aligned} \tag{22}$$

Only the cases $r=1,2$ contribute to $T^{r}(\boldsymbol{\epsilon}',\hat{\mathbf{k}}',\boldsymbol{\epsilon}'',\hat{\mathbf{k}}'')_{\mathrm{ONLD}}$. (See equations (7) and (8).) We find

$$\begin{aligned}T^{1}_{\rho}(\boldsymbol{\epsilon}',\hat{\mathbf{k}}',\boldsymbol{\epsilon}'',\hat{\mathbf{k}}'')_{\mathrm{ONLD}}&=\frac{1}{3}(\hat{\mathbf{k}}'-\hat{\mathbf{k}}'')_{\rho}+\frac{\sqrt{15}}{6}\left([[\boldsymbol{\epsilon}',\boldsymbol{\epsilon}']^{2},\hat{\mathbf{k}}']^{1}_{\rho}-[[\boldsymbol{\epsilon}'',\boldsymbol{\epsilon}'']^{2},\hat{\mathbf{k}}'']^{1}_{\rho}\right)\\&=\frac{1}{2}(\hat{\mathbf{k}}'-\hat{\mathbf{k}}'')_{\rho},\end{aligned}$$

independent of polarization, and

$$T^{2}_{\rho}(\boldsymbol{\epsilon}',\hat{\mathbf{k}}',\boldsymbol{\epsilon}'',\hat{\mathbf{k}}'')_{\mathrm{ONLD}}=-\frac{\sqrt{3}}{2}\left([[\boldsymbol{\epsilon}',\boldsymbol{\epsilon}']^{2},\hat{\mathbf{k}}']^{2}_{\rho}-[[\boldsymbol{\epsilon}'',\boldsymbol{\epsilon}'']^{2},\hat{\mathbf{k}}'']^{2}_{\rho}\right).$$

[6] The two-electron pseudoscalar does not possess a one-electron counterpart, as $\boldsymbol{\Omega}^{L}_{t}\cdot\mathbf{l}_{t}=0$.

[7] Usually, experiments are performed using two mutually perpendicular linearly-polarized states. Here we treat the general case of two linearly-polarized states making an arbitrary angle.

Effective electron operators. In equation (21), the electronic operators read

$$F^r_\rho(\omega)^{l,l',l''}_{\mathrm{ONCD}} = \sum_{\substack{\alpha\beta \\ \lambda\lambda'\lambda_1\lambda_2}} C^{r\rho}_{1\alpha,1\beta}\left[\frac{C^{l'\lambda'}_{l\lambda,1\alpha}C^{l''\lambda_1}_{l''\lambda_2,1\beta}\langle g|a^\dagger_{l'\lambda'}a_{l\lambda}a^\dagger_{l''\lambda_1}a_{l''\lambda_2}|g\rangle}{\sqrt{2l'+1}}\right.$$
$$\left. + (-1)^{r+1}\frac{C^{l''\lambda_2}_{l''\lambda_1,1\alpha}C^{l\lambda}_{l'\lambda',1\beta}\langle g|a^\dagger_{l''\lambda_2}a_{l''\lambda_1}a^\dagger_{l\lambda}a_{l'\lambda'}|g\rangle}{\sqrt{2l+1}}\right]. \tag{23}$$

Rewriting $F^r_\rho(\omega)^{l,l',l''}_{\mathrm{ONCD}}$ in the shift-operator framework of section 3, we find

$$\Sigma^{\mathrm{ONLD}}_{\mathrm{E1-M1}} = -\frac{8\pi^2\alpha}{mc}\sum_{ll'l''}R^1_{ll'}R^0_{l''l''}(-1)^\rho\left[T^1_{-\rho}(\boldsymbol{\epsilon}',\hat{\mathbf{k}}',\boldsymbol{\epsilon}'',\hat{\mathbf{k}}'')_{\mathrm{ONLD}}\right.$$
$$\times\sum_{\iota\iota'}\langle g|(\mathbf{n}_\iota\times\mathbf{l}_{\iota'}-\mathbf{l}_{\iota'}\times\mathbf{n}_\iota)_\rho|g\rangle$$
$$\left.+\mathrm{i}2\sqrt{2}T^2_{-\rho}(\boldsymbol{\epsilon}',\hat{\mathbf{k}}',\boldsymbol{\epsilon}'',\hat{\mathbf{k}}'')_{\mathrm{ONLD}}\sum_{\iota\iota'}\langle g|[\mathbf{n}_\iota,\mathbf{l}_{\iota'}]^2_\rho|g\rangle\right]. \tag{24}$$

The foregoing equation provides the required integral relation for ONLD. It accounts for two effects; namely, *magnetoelectric anisotropy* and *Jones' dichroisms*. This distinction is somehow historical; both phenomena arise from magnetoelectric configurations in the sample, which favour $\mathbf{E}\perp\mathbf{B}$ or $\mathbf{E}\parallel\mathbf{B}$ (or antiparallel), respectively[8].

Magnetoelectric anisotropy is a polarization-independent phenomenon which results from the change in the refractive index (or in the absorption coefficient) as a function of light propagation with respect to the product $\mathbf{E}\times\mathbf{B}$. It reaches its largest magnitude when the signal is recorded with the light beam parallel and antiparallel to $\mathbf{E}\times\mathbf{B}$; i.e., $\hat{\mathbf{k}}' = -\hat{\mathbf{k}}''$ in equation (24). $T^2(\boldsymbol{\epsilon}',\hat{\mathbf{k}}',\boldsymbol{\epsilon}'',\hat{\mathbf{k}}'')_{\mathrm{ONLD}} = 0$, in this case, and only the rank-1 tensor needs to be taken into account. The effect vanishes when $\mathbf{E}\parallel\mathbf{B}$ (or antiparallel). On the basis of symmetry arguments, the effect was predicted in all media whose refractive index contains a contribution of the form $\hat{\mathbf{k}}\cdot\mathbf{E}\times\mathbf{B}$ (Rikken *et al* 2002). In our integral relation, magnetoelectric dichroism is described by the two-particle *orbital anapole*: $\sum_{\iota\iota'}(\mathbf{n}_\iota\times\mathbf{l}_{\iota'}-\mathbf{l}_{\iota'}\times\mathbf{n}_\iota)$. This term can be spontaneous or induced by applying external electric and magnetic fields. Equation (21) yields a microscopic interpretation of the magnetoelectric effect recently observed $GaFeO_3$, a polar ferrimagnetic crystal (Jung *et al* 2004). $GaFeO_3$ (and in general all magnetoelectric oxides of the type $Ga_{2-x}Fe_xO_3$) is an example of a compound where spontaneous polarization and magnetization coexist. Below T_c (~ 205) the space and magnetic point groups of this crystal are $Pc2_1n$ and $m'2'm$, respectively (Kubota *et al* 2004). Note that $m'2'm$ permits a nonvanishing two-particle orbital anapole, i.e. the effective operator responsible for the effect according to our theory.

Predicted in 1948, again on the basis of symmetry arguments (Jones 1948), Jones' dichroism and birefringence were observed for the first time in 2001 (Roth and Rikken 2002). The effects are permitted in a variety of systems and compounds; for example, in uniaxial crystals, or in isotropic media when external electric and magnetic fields are applied. They are due to a difference in the imaginary and real parts of the refractive index, Δn, for linearly-polarized light at angles θ and $-\theta$ with the spontaneous magnetization (or applied external field). Jones' effects are largest when $\mathbf{E}\parallel\mathbf{B}$ (or antiparallel) and vanish for $\mathbf{E}\perp\mathbf{B}$. As depicted in figure 1, consider $\mathbf{B} = B\hat{\mathbf{z}}$ and $\hat{\mathbf{x}}$ such that $\mathbf{E} = E_x\hat{\mathbf{x}} + E_z\hat{\mathbf{z}}$. Light propagates

[8] These electric and magnetic fields, denoted by **E** and **B** respectively, can be either spontaneous, i.e., naturally present in the sample, or externally applied.

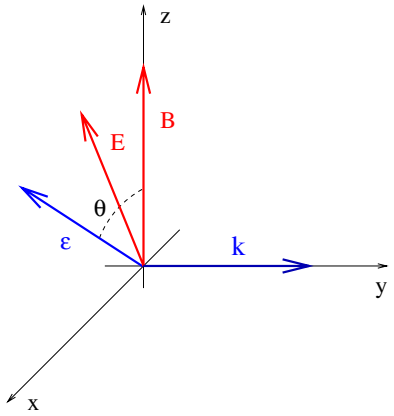

Figure 1. Experimental configuration for detecting Jones' dichroism.

along $\hat{\mathbf{y}}$ with linearly polarization at an angle θ with respect to $\hat{\mathbf{z}}$, i.e. $\boldsymbol{\epsilon}(\theta) = \sin\theta\hat{\mathbf{x}} + \cos\theta\hat{\mathbf{z}}$. In this case (Budker and Stalnaker 2003),

$$\Delta n \sim n_\theta - n_{-\theta} \propto \sin\theta\cos\theta\mathbf{E}\cdot\mathbf{B}, \tag{25}$$

which attains a maximum when $\theta = 45^\circ$ and $\mathbf{E} \parallel \mathbf{B}$ (or antiparallel). According to our integral relation, equation (24), Jones' dichroism is controlled by a two-particle *orbital magnetic quadrupole*: $\sum_{ll'}[\mathbf{n}_l, \mathbf{l}_{l'}]^2$. $[T^1(\boldsymbol{\epsilon}', \hat{\mathbf{k}}', \boldsymbol{\epsilon}'', \hat{\mathbf{k}}'')_{\mathrm{ONLD}} = 0$, for $\hat{\mathbf{k}}' = \hat{\mathbf{k}}'' = k\hat{\mathbf{y}}$, $\boldsymbol{\epsilon}' = \boldsymbol{\epsilon}(\theta)$ and $\boldsymbol{\epsilon}'' = \boldsymbol{\epsilon}(-\theta)$.] As has been demonstrated (Carra 2004), in the one-particle case, a simple Hamiltonian can be found whose ground state is an eigenstate of a magnetic quadrupole; such a ground state possesses an electric and a magnetic moment in a parallel configuration. Note that, in the configuration of figure 1, $T_0^2(\boldsymbol{\epsilon}', \hat{\mathbf{k}}', \boldsymbol{\epsilon}'', \hat{\mathbf{k}}'')_{\mathrm{ONLD}} \propto \mathrm{i}\boldsymbol{\epsilon}_0 \cdot (\boldsymbol{\epsilon} \times \hat{\mathbf{k}})_0 = \mathrm{i}\sin\theta\cos\theta$, correctly reproducing the angular dependence of Jones' dichroism. In equation (24), both electron operators are space and time odd; they have therefore *magnetoelectric* symmetry.

5. Conclusion

The current paper has derived E1–M1 integral relations for optical spectroscopies in noncentrosymmetric systems. Within a single-ion model, with hybridized valence states, we have applied angular-momentum-recoupling techniques to express integrated spectra as linear combinations of ground-state expectation values of two-particle orbital electronic tensors. Circular and linear dichroisms have been studied, and related to polar and magnetoelectric properties, respectively, of the sample.

As stressed in the introduction, our local approximation is not suitable for quantitative predictions in the optical region. However, by identifying on-site couplings between light and electrons, in the case of parity breaking, our results should help clarifying the microscopic origin of E1–M1 dichroism. For this purpose, our integral relation have been used to interpret several optical-dichroism experiments in noncentrosymmetric systems.

Acknowledgments

We are grateful to E Katz and T A L Ziman for a critical reading of the manuscript.

Appendix

The current appendix discusses algebraic details, which enter the derivation of equation (6). By resorting to spherical components, e.g.

$$\boldsymbol{\epsilon}\cdot\mathbf{r}=\sum_{q}(-1)^{q}\boldsymbol{\epsilon}_{q}r_{-q}\qquad\text{and}\qquad(\boldsymbol{\epsilon}\times\hat{\mathbf{k}})_{q}=-\mathrm{i}\sqrt{2}\sum_{\mu\nu}C^{1q}_{1\mu;1\nu}\boldsymbol{\epsilon}_{\mu}\hat{\mathbf{k}}_{\nu},\tag{A.1}$$

Equation (5) can be written as

$$\begin{aligned}\sigma^{\epsilon}_{\mathrm{E1\text{–}M1}}(\omega)=-\mathrm{i}\frac{2\sqrt{2}\pi^{2}\alpha\hbar\omega}{mc}\Bigg[&\sum_{f}\sum_{\substack{l\lambda\sigma\\ l'\lambda'\sigma'}}\sum_{\substack{l_1\lambda_1\sigma_1\\ l_2\lambda_2\sigma_2}}\sum_{\substack{qq'\\ \mu\nu}}(-1)^{q+q'}\delta_{\sigma\sigma'}\delta_{\sigma_1\sigma_2}\\ &\times R^{1}_{ll'}R^{0}_{l_1l_2}\boldsymbol{\epsilon}^{*}_{-q}C^{1-q'}_{1\mu;1\nu}\boldsymbol{\epsilon}_{\mu}\hat{\mathbf{k}}_{\nu}\frac{C^{l'\lambda'}_{l\lambda;1q}C^{l_1\lambda_1}_{l_2\lambda_2;1q'}\langle l'\|r\|l\rangle\langle l_1\|l\|l_2\rangle}{\sqrt{(2l'+1)(2l_1+1)}}\\ &\times\langle g|a^{\dagger}_{l'\lambda'\sigma'}a_{l\lambda\sigma}|f\rangle\langle f|a^{\dagger}_{l_1\lambda_1\sigma_1}a_{l_2\lambda_2\sigma_2}|g\rangle+\text{c.c.}\Bigg]\delta(E_f-E_g-\hbar\omega),\end{aligned}\tag{A.2}$$

where the Wigner–Eckart theorem has been applied to the matrix elements $\langle l'\lambda'|r_q|l\lambda\rangle$ and $\langle l_1\lambda_1|l_{q'}|l_2\lambda_2\rangle$. Implementing the identity $\sum_{r\rho}C^{r\rho}_{1q;1q'}C^{r\rho}_{1\alpha;1\beta}=\delta_{\alpha,q}\delta_{\beta,q'}$, we then consider

$$\begin{aligned}&\sum_{\substack{qq'\\ \mu\nu}}(-1)^{q+q'}C^{1-q'}_{1\mu;1\nu}C^{l'\lambda'}_{l\lambda;1q}C^{l_1\lambda_1}_{l_2\lambda_2;1q'}\boldsymbol{\epsilon}^{*}_{-q}\boldsymbol{\epsilon}_{\mu}\hat{\mathbf{k}}_{\nu}\\ &\qquad=\sum_{\substack{qq'\mu\nu\\ \alpha\beta r\rho}}(-1)^{r+\rho}C^{r-\rho}_{1-q;1-q'}C^{r\rho}_{1\alpha;1\beta}C^{1-q'}_{1\mu;1\nu}C^{l'\lambda'}_{l\lambda;1\alpha}C^{l_1\lambda_1}_{l_2\lambda_2;1\beta}\boldsymbol{\epsilon}^{*}_{-q}\boldsymbol{\epsilon}_{\mu}\hat{\mathbf{k}}_{\nu}\end{aligned}\tag{A.3}$$

and apply the recoupling transformation

$$\sum_{q'}C^{1-q'}_{1\mu;1\nu}C^{r-\rho}_{1-q;1-q'}=\sum_{p\kappa}(-1)^{r+1}\sqrt{3(2p+1)}\begin{Bmatrix}1&1&p\\1&r&1\end{Bmatrix}C^{p\kappa}_{1-q;1\mu}C^{r-\rho}_{p\kappa;1\nu}.\tag{A.4}$$

Equation (A.2) takes therefore the form

$$\begin{aligned}\sigma^{\epsilon}_{\mathrm{E1\text{–}M1}}(\omega)=\mathrm{i}\frac{2\sqrt{2}\pi^{2}\alpha\hbar\omega}{mc}\Bigg[&\sum_{f}\sum_{\substack{l\lambda\sigma\\ l'\lambda'\sigma'}}\sum_{\substack{l_1\lambda_1\sigma_1\\ l_2\lambda_2\sigma_2}}\sum_{\substack{q\mu\nu\alpha\\ \beta r\rho p\kappa}}(-1)^{\rho}\delta_{\sigma\sigma'}\delta_{\sigma_1\sigma_2}\\ &\times R^{1}_{ll'}R^{0}_{l_1l_2}\sqrt{3(2p+1)}\begin{Bmatrix}1&1&p\\1&r&1\end{Bmatrix}C^{p\kappa}_{1-q;1\mu}C^{r-\rho}_{p\kappa;1\nu}C^{r\rho}_{1\alpha;1\beta}C^{l'\lambda'}_{l\lambda;1\alpha}C^{l_1\lambda_1}_{l_2\lambda_2;1\beta}\\ &\times\boldsymbol{\epsilon}^{*}_{-q}\boldsymbol{\epsilon}_{\mu}\hat{\mathbf{k}}_{\nu}\frac{\langle l'\|r\|l\rangle\langle l_1\|l\|l_2\rangle}{\sqrt{(2l'+1)(2l_1+1)}}\langle g|a^{\dagger}_{l'\lambda'\sigma'}a_{l\lambda\sigma}|f\rangle\langle f|a^{\dagger}_{l_1\lambda_1\sigma_1}a_{l_2\lambda_2\sigma_2}|g\rangle+\text{c.c.}\Bigg]\\ &\times\delta(E_f-E_g-\hbar\omega),\end{aligned}\tag{A.5}$$

Defining the geometric factors $\mathcal{S}^{r}$ and $\mathcal{Q}^{r}$ as in equations (7)–(9), we have

$$\sigma^{\epsilon}_{\mathrm{E1\text{–}M1}}(\omega)=\mathrm{i}\frac{2\sqrt{2}\pi^{2}\alpha\hbar\omega}{mc}\Bigg\{\sum_{f}\sum_{\substack{l\lambda\sigma\\ l'\lambda'\sigma'}}\sum_{\substack{l_1\lambda_1\sigma_1\\ l_2\lambda_2\sigma_2}}\sum_{\substack{\alpha\beta\\ r\rho}}(-1)^{\rho}\delta_{\sigma\sigma'}\delta_{\sigma_1\sigma_2}$$

$$\times R^1_{ll'} R^0_{l_1 l_2} C^{r\rho}_{1\alpha;1\beta} \left[\mathcal{S}^r_{-\rho}(\boldsymbol{\epsilon}^*, \boldsymbol{\epsilon}, \hat{\mathbf{k}}) \frac{\langle l' \| r \| l \rangle \langle l_1 \| l \| l_2 \rangle}{\sqrt{(2l'+1)(2l_1+1)}} C^{l'\lambda'}_{l\lambda;1\alpha} C^{l_1\lambda_1}_{l_2\lambda_2;1\beta} \right.$$
$$\times \langle g | a^\dagger_{l'\lambda'\sigma'} a_{l\lambda\sigma} | f \rangle \langle f | a^\dagger_{l_1\lambda_1\sigma_1} a_{l_2\lambda_2\sigma_2} | g \rangle + (-1)^r \mathcal{Q}^r_{-\rho}(\boldsymbol{\epsilon}^*, \boldsymbol{\epsilon}, \hat{\mathbf{k}})$$
$$\left. \times \frac{\langle l_2 \| l \| l_1 \rangle \langle l \| r \| l' \rangle}{\sqrt{(2l+1)(2l_2+1)}} C^{l\lambda}_{l'\lambda';1\beta} C^{l_2\lambda_2}_{l_1\lambda_1;1\alpha} \langle g | a^\dagger_{l_2\lambda_2\sigma_2} a_{l_1\lambda_1\sigma_1} | f \rangle \langle f | a^\dagger_{l\lambda\sigma} a_{l'\lambda'\sigma'} | g \rangle \right]$$
$$\times \delta(E_f - E_g - \hbar\omega). \tag{A.6}$$

Finally, equation (6) is obtained from equation (A.5) by integrating over energy with use of $\sum_f |f\rangle\langle f| = 1$ and inserting well-known results for the reduced matrix elements.

References

Alagna L, Prosperi T, Turchini S, Goulon J, Rogalev A, Goulon-Ginet C, Natoli C R, Peacock R D and Stewart B 1998 *Phys. Rev. Lett.* **80** 4779

Barron L D 1982 *Molecular Light Scattering and Optical Activity* (Cambridge: Cambridge University Press)

Benoist R, Carra P and Andersen O K 2000 *Eur. Phys. J.* B **18** 193

Budker D and Stalnaker J 2003 *Phys. Rev. Lett.* **91** 263901

Carra P 2004 *J. Phys. A: Math. Gen.* **37** L183

Carra P 2001 *J. Magn. Magn. Mater.* **233** 8

Carra P and Benoist R 2000 *Phys. Rev.* B **62** R7703

Carra P, Jerez A and Marri I 2003 *Phys. Rev.* B **67** 045111

Carra P and Thole B T 1994 *Rev. Mod. Phys.* **66** 1509

Englefield M J 1972 *Group Theory and the Coulomb Problem* (New York: Wiley Interscience)

Goulon J, Goulon-Ginet C, Rogalev A, Gotte V, Malgrange C, Brouder C and Natoli C R 1998 *J. Chem. Phys.* **108** 6394

Goulon J, Rogalev A, Wilhelm F, Goulon-Ginet C, Benayoum G, Paolasini L, Brouder C, Malgrange C and Metcalf P A 2000 *Phys. Rev. Lett.* **85** 4385

Goulon J, Rogalev A, Wilhelm F, Goulon-Ginet C, Carra P, Cabaret D and Brouder C 2002 *Phys. Rev. Lett.* **88** 237401

Jones R C 1948 *J. Opt. Soc. Am.* **38** 671

Jung J H, Matsubara M, Arima T, He J P, Kaneko Y and Tokura Y 2004 *Phys. Rev. Lett.* **93** 037403

Krichevtsov B B, Pavlov V V, Pisarev R V and Gridnev V N 1996 *Phys. Rev. Lett.* **76** 4628

Kubota M, Arima T, Kaneko Y, He J P, Yu X Z and Tokura Y 2004 *Phys. Rev. Lett.* **92** 137401

Marri I and Carra P 2004 *Phys. Rev.* B **69** 113101

Natoli C R, Brouder C, Sainctavit P, Goulon J, Goulon-Ginet C and Rogalev A 1998 *Eur. Phys. J.* B **4** 1

Rikken G L J A, Strohm C and Wyder P 2002 *Phys. Rev. Lett.* **89** 133005

Roth T and Rikken G L J A 2000 *Phys. Rev. Lett.* **85** 4478

Roth T and Rikken G L J A 2002 *Phys. Rev. Lett.* **88** 063001

Varshalovich D A, Moskalev A N and Khersonskii V K 1988 *Quantum Theory of Angular Momentum* (Singapore: World Scientific)

Wagnier G and Meier A 1982 *Chem. Phys. Lett.* **93** 78